Kovove Mater. 48 2010 145–152
DOI: 10.4149/km_2010_2_145

Controllable synthesis of multiple shapes of gold nanostructures

L. Wang[1]*, L. Sun[2], Z. Li[2]

[1] *College of Chemistry, Jilin Normal University, Siping 136000, China*
[2] *State Key Laboratory of Electroanalytical Chemistry, Changchun Institute of Applied Chemistry, Chinese Academy of Sciences, Changchun 130022, China*

Received 15 July 2009, received in revised form 17 September 2009, accepted 3 November 2009

Abstract

In this work, we present a simple one-step method to synthesize various gold nanostructures (microplates, nanowires and nanowire networks) with the high yield using cinnamic acid (CA, $C_9H_8O_2$) as reducing and capping agent through a thermal process. In this reaction system, by adjusting the concentration of CA from a high level to low level, the shape of the products was found to change from nanoparticles/microplates to two-dimensional nanowire networks/branched nanowires, ultimately to one-dimensional nanowires. Additionally, the size of the products increased with the increase in the concentration of $HAuCl_4$ in the reaction system. The shape of the products was also strongly dependent on the pH of the reaction solution. By controlling the reaction time, the possible mechanism about the formation of different shape gold nanostructures was deduced.

K e y w o r d s: metal, nanostructure, crystal growth, TEM

1. Introduction

A growing research on metal nanomaterials has been mainly focused on the synthesis of nanoclusters with desired size and shape due to their potential applications in catalysis, solar energy conversion devices, chemical sensing, photonics, electronics etc. [1–4]. In relation to emerging electronic technologies, more complicated nanostructures are in demand (e.g., nanowires, nanotubes and their two-dimensional (2-D) and three-dimensional (3-D) nanoparticle assemblages). As we know, the materials with nanoscaled sizes in one, two or three dimensions have unusual physical, chemical and mechanical properties [5]. All of these advantages encourage the studies in developing new methods for the preparation of well-defined 1-D, 2-D and 3-D nanostructures.

Various methods have been employed to fabricate shape-controlled gold nanostructures, such as template methods [6–8], seed-mediated growth methods [9, 10], electrochemical [11] and photochemical methods [12, 13], etc. Recently, much attention has been focused on the fabrication of 2-D and 3-D architectures via templateless wet-chemical approaches [14–16], which have obvious advantages compared with other methods in the practical application. For example, the post-synthetic physical or chemical treatment for removing the unwanted materials (templates) is not required, which avoids the risk of destroying the morphology and structure of the products. But there are still challenges of synthesizing size-controlled nanocrystals with the novel shapes and structures, it is necessary to find new methods to synthesize complicated metal nanostructures. In our previous work [17], we selected a suitable capping agent to prepare Au nanochains, and the results indicated that cinnamic acid (CA) played a very important role for the formation of different nanostructures due to its character in structure--direction. Moreover, as an innocuous ingredient, CA can be extensively applied to various areas, such as chemical engineering, manufacture of anticancer drug, food and flavour, etc.

In this paper, we describe a facile method to prepare gold microplates, 1-D nanowires and 2-D networks of nanowires by CA reduction of hydrogen tetrachloroaurate ($HAuCl_4$) without additional capping agents by a thermal process. Fine control over the

*Corresponding author: tel.: +86-4342226609; e-mail address: yumo1002@yahoo.com.cn

shape and size of the products can be achieved by adjusting the concentration of CA or $HAuCl_4$ in the reaction system, which suggests that the molar ratio of CA to $HAuCl_4$ is a key factor for producing of different gold nanocrystals. Additionally, the shape of the products also depends on the pH of the reaction system. When the reaction solution was adjusted to alkali, the product was only spherical nanoparticles. This wet chemical method of fabricating gold nanowires and planar microplates, which are template-free, seedless and surfactant-free, may have many potential applications for the large-scale synthesis and design of future nanodevices.

2. Experimental

2.1. Materials

Cinnamic acid (CA, 99 %) was purchased from Alfa Aesar. Hydrogen tetrachloroaurate (III) ($HAuCl_4$), concentrated HCl (G. R.) and NaOH (G. R.) were supplied by Beijing chemical Reagent Co. All chemicals were used without further purification. The water used throughout the experiment was ultra pure water.

2.2. Synthesis of Au nanostructures

Au nanocrystals were prepared by using CA as a reductant to reduce $HAuCl_4$ aqueous solution. The detailed procedures were as follows: sample 1, 0.4 mL of 12 mM aqueous $HAuCl_4$ was added into 19.6 mL of 10 mM CA aqueous solution; sample 2 and 3, 1 mL and 0.25 mL of 10 mM CA aqueous solution was diluted to 19.6 mL with water, respectively, then 0.4 mL of 12 mM aqueous $HAuCl_4$ was added into above two mixtures. The molar ratio of CA to $HAuCl_4$ of the three samples was about 25 : 0.6, 25 : 12 and 25 : 48, respectively. Under reflux condition, the mixture solutions were heated at 100 ℃. The sample 1 changed its colour from pale yellow to orange with blue after it had been heated for 13 min. Sample 2 turned to light brown-red with some precipitations after it had been heated for 38 min. Sample 3 turned to light dark with some precipitations after it had been heated for 140 min. In the control experiments, the pH of CA solution was tuned to about 10 and 3 by 1 M NaOH and HCl solution, respectively, and other procedure was the same as that of sample 1. Then the reaction solution was heated at 100 ℃.

2.3. Characterization

The as-prepared Au nanocrystals solution was investigated on Cary-500 UV-vis spectrometer (VARIAN, USA). The morphology of the products was characterized with a JEOL-1011 transmission electron microscope (TEM) at an accelerating voltage of 100 kV. The samples for TEM measurements were prepared by casting a drop of the as-prepared Au suspensions onto a carbon-coated copper grid, then allowing it to dry in air. The sample after TEM characterization was then imaged by an XL30 ESEM FEG field emission scanning electron microscopy (SEM, FEI Company) at an accelerating voltage of 20 kV. The X-ray photoelectron spectroscopy (XPS) analysis of the product was conducted using a PHERMO ESCALAB 250 spectrometer.

3. Results and discussion

3.1. The influence of the concentration of CA on the products shape

The crystal structure of the products was first investigated by TEM. When the molar ratio of CA to $HAuCl_4$ is 25 : 0.6, the as-prepared product is quasi-spherical nanoparticles with some microplates as shown in Fig. 1a. When the molar ratio is decreased to 25 : 12, the product is a mainly 2-D network of nanowires with a uniform diameter of ø 40 nm in a high yield (Fig. 1b). The inset shows SEM images of the nanowire networks that were taken at a tilting angle of 45°. The wires are flat and oriented parallel to the surface of the supporting substrate. Figure 1c presents a higher magnification view from the selected area of Fig. 1b. This image shows that the product is not linear aggregate of nanoparticles but continuous wires with 2-D networks. The inset shows the related selected area electron diffraction (SAED) pattern obtained by aligning the electron beam perpendicular to the planar surface of nanowire, the hexagonal symmetry diffraction spots pattern indicates that the wire is a single crystal [14, 18–20]. This result suggests that each wire of nanowire networks is, in fact, a nanobelt (or ribbon) characterized by a single crystalline structure [20]. The XPS spectrum of this product shows that the binding energy of Au $4f_{7/2}$ and Au $4f_{5/2}$ appear at 83.35 eV and 87.05 eV, respectively, agreeing with that of Au^0 as shown in Fig. 2, which indicates the nanowire networks are composed of elemental gold [21]. As the molar ratio is decreased to 25 : 48, the product was 1-D nanowires in large quantities with a typical diameter ranging from 20 nm to 30 nm (Fig. 1d). The length of wires is up to tens of micrometers. The inset (up) gives that the enlarged view of a part of the selected nanowires, revealing the continuity of wires. The inset (down) exhibits the corresponding SAED pattern of the 1-D nanowires, indicating the formation of face-centred cubic (fcc) nanocrystals. The above results demonstrate that the shape of the products obtained by our method can be controlled by adjusting the concentration of CA.

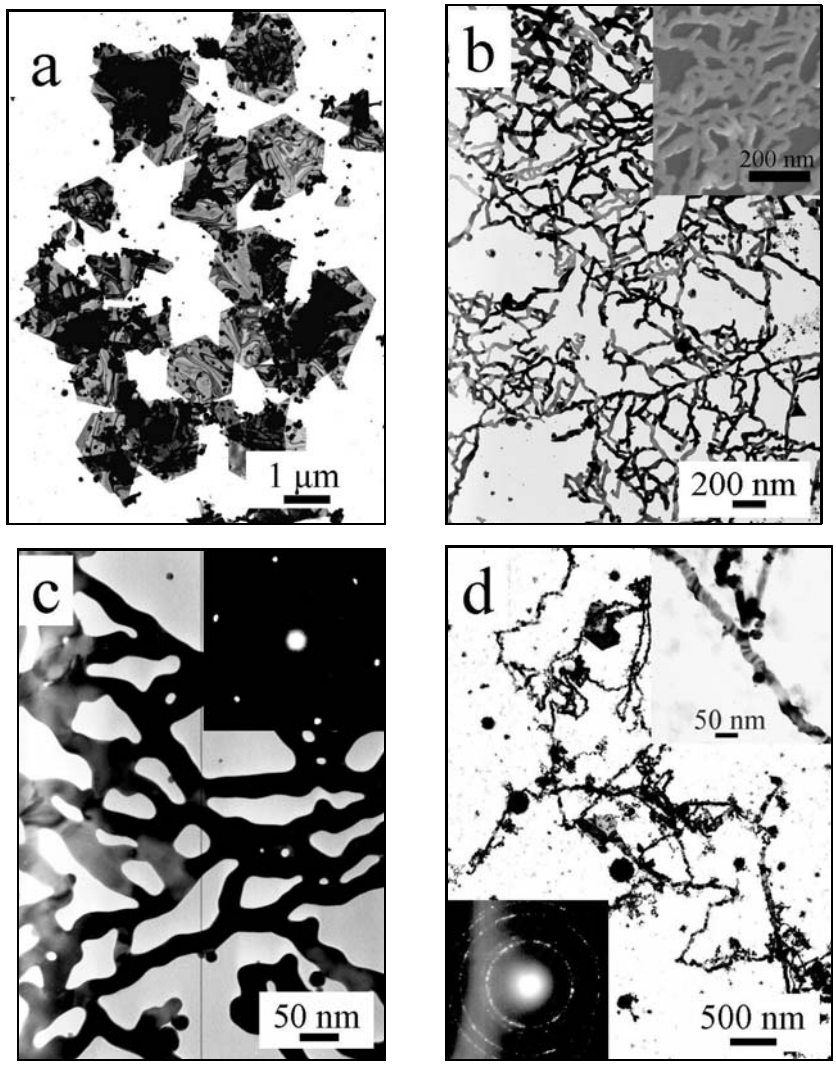

Fig. 1. TEM images of Au nanostructures synthesized by adjusting the molar ratio of CA to $HAuCl_4$ as (a) 25 : 0.6, (b), (c) 25 : 12, (d) 25 : 48, respectively, (c) is a magnified image of (b). The inset SEM image in (b) was taken at a tilting angle of 45°, and the inset images in (c) and (d) reveal the related electron diffraction patterns.

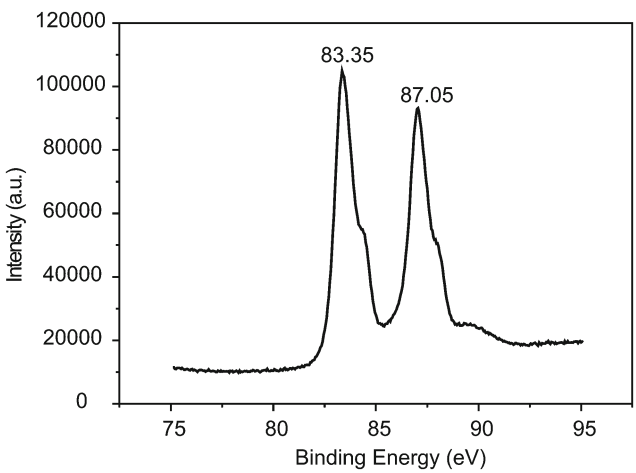

Fig. 2. XPS analysis of Au 4f orbital of the as-prepared product obtained from the molar ratio of CA to $HAuCl_4$ at 25 : 12.

The UV-vis spectroscopic method can be used to track the morphological evolution because Au nanostructures with different shapes can give surface plasmon resonance (SPR) bands at different frequencies. Figure 3 shows the UV-vis absorption spectra of three as-prepared colloidal suspensions prepared. When the molar ratio is 25 : 0.6, the spectrum gives two plasmon absorption bands located at about 606 and 920 nm, indicating the formation of Au nanostructures (Fig. 3a) [19]. It is well known that spherical Au particles show a transverse plasmon absorption band at approximately 520 nm, and this band is usually red-shifted to longer wavelength with the increase of particle size [22]. The microplates give two absorption bands in its UV-vis spectrum, transverse and longitudinal plasmon band [14]. Therefore, the absorption band at 606 nm may be attributed to the superposition of transverse plasmon resonances of nanoparticles and longitudinal plasmon

resonances of microplates at relevant wavelengths [19]. Obviously, the absorption band at 920 nm originates from the longitudinal plasmon resonance of Au microplates [19, 23]. The bands are broad because of the relatively high polydispersity in size. As the molar ratio is decreased to 25 : 12, an almost-flat absorption curve with a relatively broad band from 500 nm to 700 nm and a rising tail of the spectrum (above 700 nm) are observed in Fig. 3b. Wang et al. reported that the network-like Au nanostructures in its UV--vis spectrum exhibited a long rising feature from visible to near-IR region [24]. Our findings are very similar with their spectrum. It is documented that Au nanorods are characterized by two bands of plasmon resonance, one is transverse plasmon band, and the other is longitudinal one depending on the aspect ratio [22]. However, in the present case Au nanowires form a network-like structure, the nanowire networks show a flat absorption pattern with a broad band in its UV-vis spectrum, which may be ascribed to the superposition of longitudinal plasmon resonances of Au nanowires with different aspect ratios [15]. No visible transverse resonance band in the spectrum is likely due to the superposition of transverse plasmon resonances of Au nanowires with different aspect ratios. When the molar ratio is 25 : 48, the absorption curve is nearly flat with a relatively broad band from 500 nm to 900 nm (Fig. 3c). Based on the discussion above, the appearance of this absorption curve is also attributed to the superposition of longitudinal plasmon resonances of Au 1-D nanowires with different aspect ratios at relevant wavelengths.

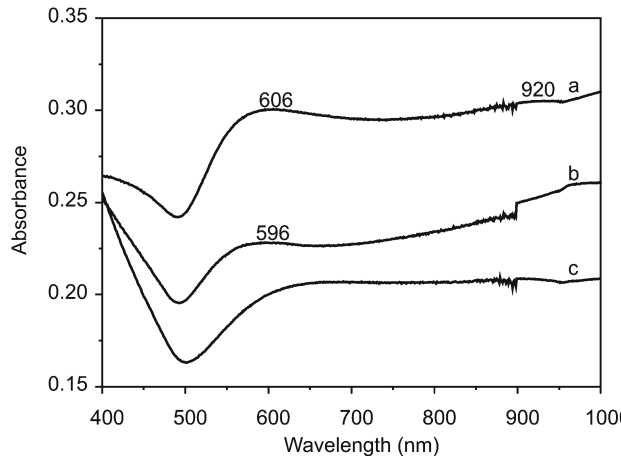

Fig. 3. UV-vis spectra of the Au suspended solution prepared by tuning the molar ratio of CA to $HAuCl_4$ as (a) 25 : 0.6, (b) 25 : 12 and (c) 25 : 48, respectively.

3.2. The influence of the concentration of $HAuCl_4$ in the reaction system and the pH of reaction solution on the morphology of the products

The size and shape of Au nanocrystals are found to strongly depend on the concentration of $HAuCl_4$ in the reaction system. In a control experiment, the amount of $HAuCl_4$ was increased from 0.4 mL to 0.8 mL, and other conditions were kept the same as those described in the experimental section. Here, the molar ratio of CA to $HAuCl_4$ was 25 : 1.2, 25 : 24 and 25 : 96, respectively. Figure 4 shows TEM images of the as--prepared Au nanostructures. When the molar ratio is 25 : 1.2, the product is dominated by large hexagonal and truncated triangular micrometer-scale Au plates (Fig. 4a). They have very sharp and smooth edges with the average edge length of 2.6 μm for hexagonal microplates and 2.7 μm for truncated triangular microplates. The lower contrast observed for the microplates suggests that they are flat and thin, unlike the nanospheres around them. The textures can be seen across the faces of the flat crystals, always extending from spots and radiating down to the edges of the plates, may be ascribed to the bending of the thin crystals or the presence of multiply twinned structures [14, 25]. As the molar ratio is 25 : 24, the product is mainly branched nanowires with the length of several micrometers as shown in Fig. 4b. The lower contrast observed for the nanowires suggests that they are flat and thin. When the molar ratio is decreased to 25 : 96, the product is mainly wire-like structures (Fig. 4c). Though there are very little branches on the ends of some wires, on the whole the structures are considered as 1-D nanowires because the wires are very long. Their length is up to 30 μm. The insets of Fig. 4a,b show the SAED patterns of related nanostructures by directing the electron beam perpendicular to the planar surface of nanocrystal, the hexagonal symmetry diffraction patterns spots demonstrate that the nanostructures are single crystals bounded mainly by {111} facets. (UV-vis spectra of three samples are shown in Fig. S of the Supporting information.) The above results indicate that the size of Au nanostructures increases with the increase in the concentration of $HAuCl_4$ in the reaction system.

The shape of the products is also dependent on the pH of reaction solution. When the pH of CA solution was adjusted to 10, the product obtained was only quasi-spherical particles with the average diameter of 15 nm as shown in Fig. 4d. (UV-vis spectrum of this sample is shown in Fig. S of the Supporting information.) The result reveals that the pH of reaction solution strongly influences the product shape. When the pH was 10, nearly all of CA (pKa = 4.46) was deprotonated, which led to the formation of thick coating over the entire surface of a particle [17]. Therefore, the selectivity of the interaction between CA and various crystallographic planes lost, and anisotropic growth of the particles could not be induced. These resulted in isotropic growth for all different faces, and thus the

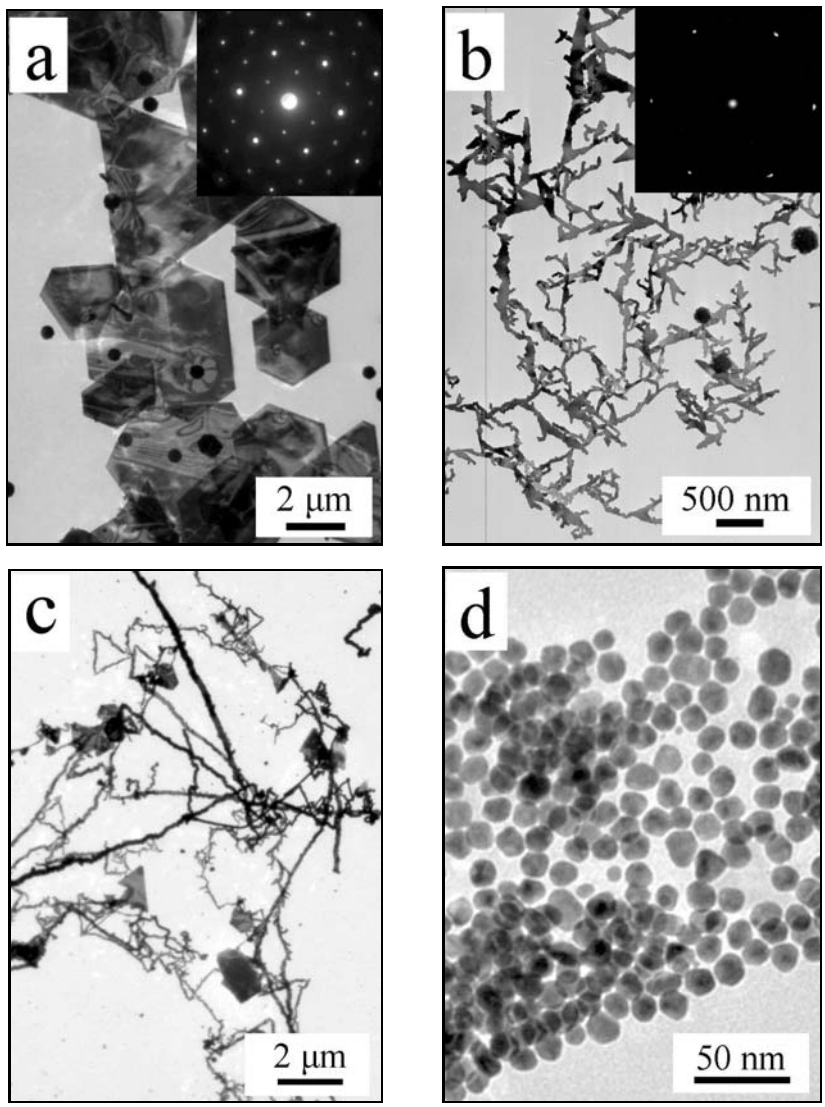

Fig. 4. TEM images of the as-prepared Au nanocrystals prepared by varying the molar ratio of CA to $HAuCl_4$ as (a) 25 : 1.2, (b) 25 : 24 and (c) 25 : 96, respectively. (d) TEM images of the nanoparticles obtained from tuning the pH of CA solution to about 10. (The insets show the related electron diffraction patterns.)

quasi-spherical nanoparticles with the uniform diameter were produced. When the pH was adjusted to 3, the colour of the reaction solution did not change after the solution had been heated for 60 min. This phenomenon indicated that Au nanostructures could not be formed under this condition.

3.3. Formation mechanism of the well-defined gold nanocrystals

On the basis of the above results, the formation of the microplates and nanowires may be attributed to the specific interaction between CA and gold crystal lattice structure. Here, CA serves as reducing and stabilizing agent. CA varies the surface energies of different crystal faces by preferentially interacting with specific planes of the particles, by which CA can control the growth rates of various faces of Au cores for tuning the shape of the particles [10]. Since Au {111} facets have the lowest surface-free energy, CA is dynamically adsorbed and desorbed on the crystal facets other than {111} planes [26, 27]. Additionally, CA as reductant bonds onto the special facets, which increases the chemically reducing environment within the local region. So the selective interaction enhances the growth rate along the specific facet direction. Therefore, the formation of Au microplates is attributed to the lowest growth rate along the {111} direction. TEM studies showed that at the initial reaction stage, with the assistance of CA, some triangular particles with small sizes (about 5–15 nm) were formed, and then they acted as the seeds. With the consumption of the smaller spherical particles, these triangular particles grew into the larger regu-

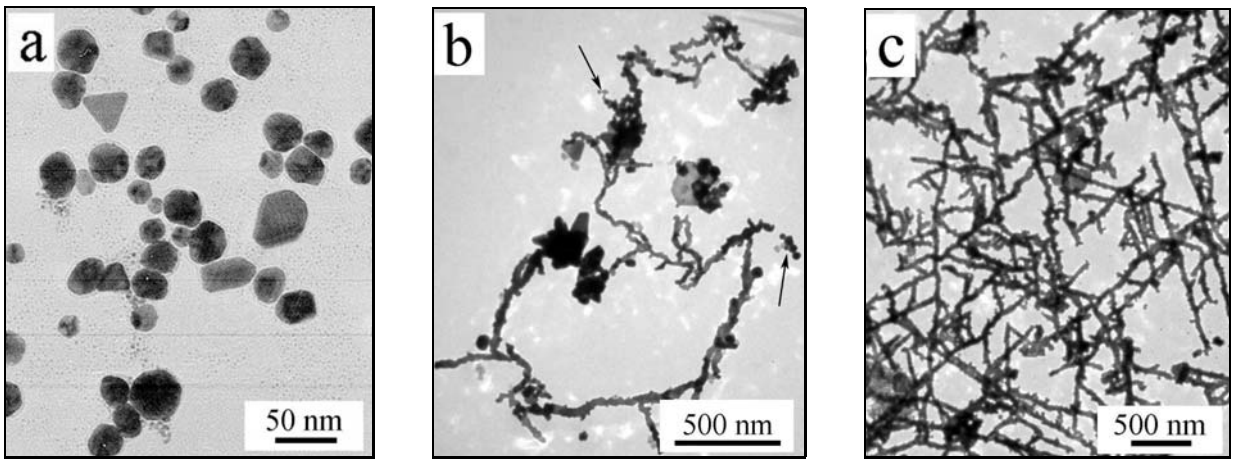

Fig. 5. TEM images of three samples, showing different stages of growth for Au nanowire networks. The samples were taken from the reaction mixture after heated for (a) 20, (b) 23 and (c) 29 min, respectively.

lar shape microplates (Ostwald's ripening) [15, 20, 28, 29].

To understand the formation mechanism of 2-D Au nanowire networks, the Au nanostructures at various stages of growth process were characterized using TEM. Figure 5 shows TEM images of the Au nanostructures that were taken from the reaction mixture after the sample 2 had been heated for 20, 23 and 29 min. These images clearly show the evolution of Au nanocrystals from 0-D into 2-D morphology over time. Figure 5a shows the initial product: a mixture of Au nanoparticles with two distinctive sizes. Some particles have the size of < 5 nm, and others are larger (10–50 nm in diameter). The nanoparticles with small size have ability to align and fuse into the existing crystal lattice [30]. When the reaction solution was continuously heated, the large nanoparticles could spontaneously assemble into chain-like structures with fractal features (see arrow in Fig. 5b). At the same time, the smaller nanoparticles were no longer stable because their surface energies are higher than those of large ones. They gradually dissolved and diffused onto the concave regions of the interconnected particles via Ostwald's ripening process, and thus the nanowires were formed (Fig. 5b) [15, 31–33]. With the elongation of the reaction time, the large particles gradually fused onto the nanowires to make the wires lengthen or to become the branches (Fig. 5c). In the process of fusion growth, the large particles maybe rearranged to monocrystal wire-like structures. With the reaction proceeding, both the length and number of Au nanowire networks increased. The growth process of the 2-D networks completely accords with the theory called Cayley tree, generated as follows: the end of each branch is a growth site from which z branches of unit length grow out. Repeating indefinitely the growth process leads to the formation of a hierarchical structure [34–36]. It can be observed from Fig. 2b that some of branches have dead ends. When two growing branches encounter each other at their ends, they stop growing and gradually form closed rings, which leads to the formation of the nanowire networks.

When the molar ratio of CA to $HAuCl_4$ was continuously decreased, the larger nanoparticles in the initial reaction stage could easily self-assemble into 1-D chain-like structures without fractal features [17, 37], so the final products were 1-D nanowires. It might be adverse to the formation of Cayley tree structures, when the amount of CA in the reaction system was very little. With the increase of the amount of $HAuCl_4$ added into the reaction system, the growth velocity of crystals was also faster because of the higher monomer concentration, and thus the larger nanocrystals were formed [25]. Herein, CA shows an excellent ability of controlling the morphology of the products.

4. Conclusions

In summary, for the first time we report a one-step method to synthesize Au nanowires and well-defined nanoparticles by directly heating a mixture solution containing CA and $HAuCl_4$. The results show that the shape and size of the Au nanocrystals synthesized by our method can be controlled by systematic variation of the experimental parameters, including the concentration of CA or $HAuCl_4$ in the reaction solution, and the pH of reaction solution. The yield of regular-shape nanocrystals is high, and relatively few spherical nanoparticles by-products are observed. The strategy to construct 1-D nanowires, 2-D nanowire network and microplates in our present work may open up an effective way to synthesize metal nanocrystals with desired shape for the fundamental study and practical application.

References

[1] BURDA, C.—CHEN, X.—NARAYANAN, R.—EL-SAYED, M. A.: Chem. Rev., *105*, 2005, p. 1025. PMid:15826010, doi:10.1021/cr030063a

[2] TIAN, C.—MAO, B.—WANG, E.—KANG, Z.—SONG, Y.—WANG, C.—LI, S.—XU, L.: Nanotechnology, *18*, 2007, p. 285607. doi:10.1088/0957-4484/18/28/285607

[3] WILLNER, I.—BARON, R.—WILLNER, B.: Adv. Mater., *18*, 2006, p. 1109. doi:10.1002/adma.200501865

[4] SUN, X.—HAGNER, M.: Langmuir, *23*, 2007, p. 9147. PMid:17650017, doi:10.1021/la701519x

[5] CHEN, C.—WANG, L.—JIANG, G.—YU, H.: Rev. Adv. Mater. Sci., *11*, 2006, p. 1.

[6] MINELLI, C.—HINDERLING, C.—HEINZELMANN, H.—PUGIN, R.—LILEY, M.: Langmuir, *21*, 2005, p. 7080. PMid:16042426, doi:10.1021/la050757+

[7] ZHANG, D.—QI, L.—YANG, J.—MA, J.—CHENG, H.—HUANG, L.: Chem. Mater., *16*, 2004, p. 872. doi:10.1021/cm0350737

[8] FULLAM, S.—COTTELL, D.—RENSMO, H.—FITZMAURICE, D.: Adv. Mater., *12*, 2000, p. 1430. doi:10.1002/1521-4095(200010)12:19<1430::AID-ADMA1430>3.0.CO;2-8

[9] JANA, N. R.—GEARHEART, L.—MURPHY, C. J.: J. Phys. Chem. B, *105*, 2001, p. 4065. doi:10.1021/jp0107964

[10] SAU, T. K.—MURPHY, C. J.: J. Am. Chem. Soc., *126*, 2004, p. 8648. PMid:15250706, doi:10.1021/ja047846d

[11] LIU, J.—DUAN, J. L.—TOIMIL-MOLARES, M. E.—KARIM, S.—CORNELIUS, T. W.—DOBREV, D.—YAO, H. J.—SUN, Y. M.—HOU, M. D.—MO, D.—WANG, Z. G.—NEUMANN, R.: Nanotechnology, *17*, 2006, p. 1922. doi:10.1088/0957-4484/17/8/020

[12] KIM, F.—SONG, J. H.—YANG, P.: J. Am. Chem. Soc., *124*, 2002, p. 14316. PMid:12452700, doi:10.1021/ja028110o

[13] ESUMI, K.—MATSUHISA, K.—TORIGOE, K.: Langmuir, *11*, 1995, p. 3285. doi:10.1021/la00009a002

[14] SHAO, Y.—JIN, Y.—DONG, S.: Chem. Comm., 2004, p. 1104.

[15] PEI, L.—MORI, K.—ADACHI, M.: Langmuir, *20*, 2004, p. 7837. PMid:15323538, doi:10.1021/la049262v

[16] RAMANATH, G.—D'ARCY-GALL, J.—MADDANIMATH, T.—ELLIS, A. V.—GANESAN, P. G.—GOSWAMI, R.—KUMAR, A.—VIJAYAMOHANAN, K.: Langmuir, *20*, 2004, p. 5583. PMid:15986704

[17] WANG, L.—WEI, G.—SUN, L.—LIU, Z.—SONG, Y.—YANG, T.—SUN, Y.—GUO, C.—LI, Z.: Nanotechnology, *17*, 2006, p. 2907. doi:10.1088/0957-4484/17/12/014

[18] SUN, X.—DONG, S.—WANG, E.: Langmuir, *21*, 2005, p. 4710. PMid:16032893, doi:10.1021/la047267m

[19] SUN, X.—DONG, S.—WANG, E.: Angew. Chem. Int. Ed., *43*, 2004, p. 6360. PMid:15558691, doi:10.1002/anie.200461013

[20] SUN, Y.—MAYERS, B.—XIA, Y.: Nano Lett., *3*, 2003, p. 675. doi:10.1021/nl034140t

[21] HÜFNER, S.: Photoelectron Spectroscopy. 2nd Ed. New York, Springer-Verlag 1996.

[22] LINK, S.—EL-SAYED, M. A.: J. Phys. Chem. B, *103*, 1999, p. 8410. doi:10.1021/jp9917648

[23] MALIKOVA, N.—PASTORIZA-SANTOS, I.—SCHIERHORN, M.—KOTOV, N. A.—LIZ-MARZAN, L. M.: Langmuir, *18*, 2002, p. 3694. doi:10.1021/la025563y

[24] CHEN, C. D.—YEH, Y. T.—WANG, C. R. C.: J. Phys. Chem. Solids, *62*, 2001, p. 1587. doi:10.1016/S0022-3697(01)00098-1

[25] BROWN, S.—SARIKAYA, M.—JOHNSON, E.: J. Mol. Biol., *299*, 2000, p. 725. PMid:10835280 doi:10.1006/jmbi.2000.3682

[26] HU, J.—CHEN, Q.—XIE, Z.—HAN, G.—WANG, R.—REN, B.—ZHANG, Y.—YANG, Z.—TIAN, Z.: Adv. Funct. Mater., *14*, 2004, p. 183. doi:10.1002/adfm.200304421

[27] CHEN, Y.—GU, X.—NIE, C.—JIANG, Z.—XIE, Z.—LIN, C.: Chem. Comm., 2005, p. 4181.

[28] LOFTON, C.—SIGMUND, W.: Adv. Funct. Mater., *15*, 2005, p. 1197. doi:10.1002/adfm.200400091

[29] JIN, R.—CAO, Y.—MIRKIN, C. A.—KELLEY, K. L.—SCHATZ, G. C.—ZHENG, J. G.: Science, *294*, 2001, p. 1901. PMid:11729310, doi:10.1126/science.1066541

[30] VASILEV, K.—ZHU, T.—WILMS, M.—GILLIES, G.—LIEBERWIRTH, I.—MITTLER, S.—KNOLL, W.—KREITER, M.: Langmuir, *21*, 2005, p. 12399. PMid:16343020, doi:10.1021/la052354f

[31] SUN, Y.—YIN, Y.—MAYERS, B. T.—HERRICKS, T.—XIA, Y.: Chem. Mater., *14*, 2002, p. 4736. doi:10.1021/cm020587b

[32] SUN, Y.—GATES, B.—MAYERS, B.—XIA, Y.: Nano Lett., *2*, 2002, p. 165. doi:10.1021/nl010093y

[33] ROOSENM, A. R.—CARTER, W. C.: Physica A, *261*, 1998, p. 232.

[34] VANDEWALLE, N.—AUSLOOS, M.: Phys. Rev. E, *55*, 1997, p. 94. doi:10.1103/PhysRevE.55.94

[35] LIU, X. Y.—SAWANT, P. D.: Appl. Phys. Lett., *79*, 2001, p. 3518. doi:10.1063/1.1415609

[36] WEI, G.—NAN, C.—DENG, Y.—LIN, Y.: Chem. Mater., *15*, 2003, p. 4436. doi:10.1021/cm034628v

[37] GIERSIG, M.—PASTORIZA-SANTOS, I.—LIZ-MARZÁN, L. M.: J. Mater. Chem., *14*, 2004, p. 607. doi:10.1039/b311454f

Supporting information

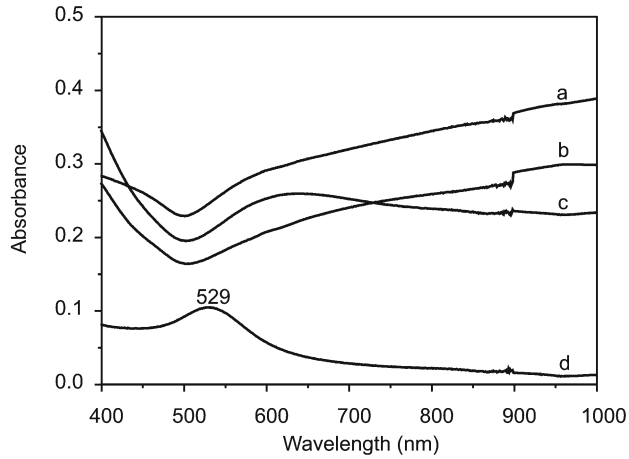

Fig. S. UV-vis spectra of the Au suspensions prepared by varying the molar ratio of CA to $HAuCl_4$ as (a) 25 : 1.2, (b) 25 : 24 and (c) 25 : 96, respectively. (d) UV-vis spectrum of the nanoparticles solution obtained from tuning the pH of CA solution to about 10.